



ARTICLE



## Fractional interpolation and multirate technique-based design of optimum IIR integrators and differentiators

Om Prakash Goswami<sup>a</sup>, Tarun K. Rawat<sup>b</sup> and Dharmendra K. Upadhyay<sup>b</sup>

<sup>a</sup>Division of Electronics and Communication Engineering, Faculty of Technology, University of Delhi, New Delhi, India; <sup>b</sup>Netaji Subhas University of Technology, New Delhi, India

### ABSTRACT

In this paper, new designs of infinite impulse response digital integrators are presented. Transfer functions of the digital integrators are derived after utilising the concept of multirate technique in the fractional interpolation of the rectangular and bilinear transform. Thereafter, the unknown variables of the obtained generalised transfer functions are optimised by using the optimisation algorithm. This yields the mean relative magnitude error,  $-63.439$  dB and  $-78.771$  dB for the first- and second-order, respectively. Furthermore, new designs of the first- and second-order digital differentiators are obtained by inverting the generalised transfer functions of the proposed integrator designs followed by optimisation of the unknown variables. The mean relative magnitude errors for first- and second-order differentiators are obtained as  $-56.478$  dB and  $-75.095$  dB, respectively. The proposed designs of integrators and differentiators exhibit the precise approximation of the ideal integrator and differentiator over the full Nyquist interval.

### ARTICLE HISTORY

Received 6 May 2020  
Accepted 27 October 2020

### KEYWORDS

Fractional bilinear transform; fractional interpolation; multirate technique; optimised digital integrators; digital differentiators

## 1. Introduction

Digital integrators and differentiators are extensively applied to find the time integral and time derivative, respectively, for either measured or input excitations. They possess diverse applications as a basic building block in the field of signal processing, instrumentation and in communication systems. Hence, the approximation of the ideal integrator and differentiator should be explicit in terms of their frequency responses (Jang & Chicharo, 1993; Liu et al., 1991; Xu et al., 2010). The frequency response of the ideal integrator is given by

$$H_{int}(\omega) = \frac{1}{j\omega} \quad (1)$$

The frequency response of the ideal differentiator is given by

$$H_{diff}(\omega) = j\omega \quad (2)$$

where  $j = \sqrt{-1}$  and  $\omega$  is the angular frequency in radians. The approach of designing digital integrator and differentiator systems can be either finite impulse response (FIR) or infinite impulse response (IIR). FIR systems have a linear phase with guaranteed stability. But, typically for the same magnitude response specifications, the order of the resulting IIR systems is much lesser than the order of the corresponding FIR systems (Oppenheim et al., 1999). Therefore, IIR systems offer several benefits in terms of fast response and fewer memory requirements.

The conventional approach to design the IIR digital integrator and differentiator is by employing the first-order approximation of the natural logarithmic function (Dyer & Dyer, 2000). It is generally termed as the bilinear transform and it accurately estimates the ideal integrator and differentiator in the low-frequency region. Pei and Hsu used the concept of fractional delay filter in the bilinear transform (Pei & Hsu, 2008). Consequently, the magnitude responses of the estimated digital integrators and differentiators have been correlated up to the wider band of their analog counterparts as compared to the bilinear transform. In 1998, Al-Alaoui used the linear interpolation between the standard rectangular and trapezoidal rule and introduced wideband digital integrators and differentiators (Al-Alaoui, 1992, 1993). Furthermore, in 2019, Goswami et al. extended the matching magnitude of digital differentiators by utilising the concept of fractional delay in the linear interpolated rectangular and trapezoidal rule (Goswami et al., 2019, 2020).

Apart from the mentioned techniques, various optimisation algorithms and approximation techniques are used to design the digital integrators and differentiators, which provide the noteworthy correlation with less relative errors with Equations (1) and (2) respectively, up to the full Nyquist band (Al-Alaoui, 1994; Al-Alaoui & Baydoun, 2013; Gupta et al., 2010a, 2010b; Stani et al., 2020; Mishra et al., 2019; Tsai et al., 2006; Upadhyay, 2010; Upadhyay & Singh, 2011).

Al-Alaoui introduced the design of a second-order integrator and differentiator after exercising the numerical integration rules followed by the optimisation in 2014 (Al-Alaoui, 2011). Nam Ngo introduced the third-order integrator and differentiator based on the Newton-Cotes integration method (Ngo, 2006). Likewise, optimisation of the pole-zero locations was used by Upadhyay to suggest wideband differentiator and integrator in 2012 (Upadhyay, 2012). Moreover, in 2017, an optimal design of IIR digital differentiators is exhibited by Aggarwal et al. after utilising bat algorithm. (Aggarwal et al., 2017). The methods mentioned above are used to design full-band digital differentiators and integrators. But, they approximate the corresponding ideal responses either by compromising the low-order or by exhibiting the substantial error in the magnitude responses.

In this paper, generalised first- and second-order digital integrator are designed by utilising the concept of the multirate technique in the fractional interpolation of bilinear and rectangular transform. The approach of multirate technique utilises the fractional delay based system with reference to the sample clock to obtain the extension in matching magnitude. The inversion of these resultant transfer functions leads to the generalised transfer function of differentiators. Thereafter both generalised equations of digital integrator and differentiator are optimised for the weighting variable  $\alpha$  and fractional delay variable  $\delta$ . These designs provide the least relative errors as compared to the existing designs. Some statistical results also calculated to support this fact.

The rest of this paper is prepared as follows: Section II outlines the application of fractional delay to the bilinear transform. Section III manifests the proposed design of the

first- and second-order integrators using fractional interpolation with utilising the multirate technique. Section IV discusses the simulation results for the proposed design of the first- and second-order integrators. Section V describes the proposed design of the first- and second-order differentiators. Section VI addresses the simulation results for the proposed design of the first- and second-order differentiators. Section VII compares the proposed designs of the integrator and differentiator with existing designs. Section VIII concludes the paper.

## 2. Motivation

Conventionally, the digital integrators have been designed by inverting the transfer function of the first-order bilinear transform. Since the bilinear transform maps the analog domain to the digital domain without losing their stability. The transfer function of the bilinear transform-based integrator is given by (Dyer & Dyer, 2000; Oppenheim et al., 1999).

$$\frac{1}{s} = \frac{T}{2} \frac{1+z^{-1}}{1-z^{-1}} \quad (3)$$

where  $T$  is the sampling time. Substitution of  $s=j\Omega$  and  $z=e^{j\omega}$  yields

$$\frac{1}{j\Omega} = \frac{T}{2} \frac{1+e^{-j\omega T}}{1-e^{-j\omega T}} = \frac{T}{2} \left( j \tan \frac{\omega T}{2} \right)^{-1} \quad (4)$$

Using the concept of fractional delay in bilinear transform, the fractional bilinear transform (FBLT) (Pei & Hsu, 2008) is described by

$$F_{frac}(z) = \frac{\delta T}{2} \frac{1+z^{-\delta}}{1-z^{-\delta}} = \frac{\delta T}{2} \left( j \tan \frac{\omega \delta T}{2} \right)^{-1} \quad (5)$$

where  $\delta$  is the fractional delay variable,  $0 \leq \delta \leq 1$  and  $T$  is taken as 1. Suitable modification in the conventional fractional delay of the FBLT, along with the multirate technique can be used to design digital integrator and differentiator.

## 3. Proposed design of the first- and second-order integrators

The proposed design is obtained by implementing the fractional interpolation between trapezoidal and rectangular rules using the concept of fractional delay used in fractional bilinear transform. Then, the multirate technique is used to extend its bandwidth to approximate the ideal integrator precisely.

### 3.1. Fractional interpolation technique

The interpolation technique employed between trapezoidal and rectangular integration results in (Al-Alaoui, 1992, 1993)

$$H(z) = aH_R(z) + (1-a)H_T(z) \quad (6)$$

where  $a$  is the weighting variable ranges  $0 \leq a \leq 1$  and  $H_R(z)$  and  $H_T(z)$  are the rectangular and trapezoidal rule-based transfer functions, respectively. It yields

$$\frac{1}{s} = \frac{T(1+\alpha) + (1-\alpha)z^{-1}}{2(1-z^{-1})} = \frac{T(1+\alpha)}{2} \left[ \frac{1 + \frac{(1-\alpha)}{(1+\alpha)}z^{-1}}{1-z^{-1}} \right] \quad (7)$$

Introducing the concept of fractional delay (Devate et al., 2014; Laakso et al., 1996) by replacing  $z^{-1}$  by  $z^{-\delta}$  in Equation (7) results in the following

$$F(z) = \frac{\delta T(1+\alpha)}{2} \left[ \frac{1 + \frac{(1-\alpha)}{(1+\alpha)}z^{-\delta}}{1-z^{-\delta}} \right] \quad (8)$$

where  $0 \leq \delta \leq 1$  and  $0 \leq \alpha \leq 1$ . Subsequently, using an approximation to the fractional delay for its equivalent integer delay (Laakso et al., 1996), the generalised transfer function of the first-order integrator is obtained as (Goswami et al., 2020)

$$F_{intel}(z) = \frac{T(1+\alpha)}{2} \left[ \frac{1 + \frac{1-\alpha}{1+\alpha}(1-\delta) + \frac{1-\alpha}{1+\alpha}\delta z^{-1}}{1-z^{-1}} \right] \quad (9)$$

The generalised transfer function of the second-order digital integrator is given by (Goswami et al., 2020)

$$F_{intez}(z) = \frac{T}{2} \left[ \frac{\delta(1-\alpha)(\delta-1) + (4-2\delta^2(1-\alpha))z^{-1} + \delta(1+\delta)(1-\alpha)z^{-2}}{(1-\delta) + 2\delta z^{-1} - (1+\delta)z^{-2}} \right] \quad (10)$$

The generalised transfer functions obtained in Equations (9) and (10) have two variables  $\alpha$  and  $\delta$ . They can be optimised to get the first- and second-order transfer function of the digital integrator. However, to approximate the proposed integrator to ideal accurately, the optimisation should be done along with the extension of their bandwidth.

### 3.2. Extension of the bandwidth of digital integrators

The bandwidth of the aforementioned generalised transfer functions is extended by applying the concept of multirate technique as shown in Figure 1 (Devate et al., 2015,

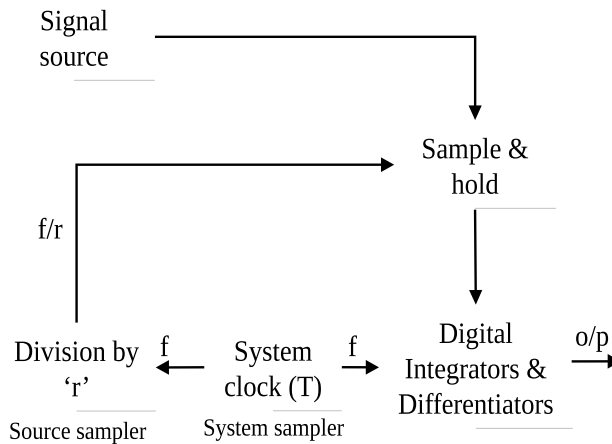


**Figure 1.** Extension of the digital bandwidth.

2014; Laakso et al., 1996). The system clock provides the clock with frequency  $f$  and time period  $T$ . It gets divided into two clocks. One clock is used to sample the signal with frequency  $f$ , and other clock determines the system delay  $z'^{-1}$  where  $z'=z^{1/r}$ . It provides the new down sampling frequency as  $f/r$ . Here, the binary divider chain is used to divide the frequency by the factor of  $r$ . The acquired low-frequency clock samples the signal from the signal source. This sampled response is again re-sampled by the system clock with a clock frequency  $f$ . This results in the extension of the digital bandwidth of the corresponding magnitude responses. Therefore, the generalised equation for the first-order integrator is obtained as

$$F_{int1}(z') = \frac{T(1+a)}{2r} \left[ \frac{1 + \frac{1-a}{1+a}(1-\delta) + \frac{1-a}{1+a}\delta z'^{-1}}{1 - z'^{-1}} \right] \Bigg|_{z'=e^{j\omega/r}} \quad (11)$$

The generalised equation for the second-order integrator is obtained as

$$F_{int2}(z') = \frac{T}{2r} \left[ \frac{\delta(1-a)(\delta-1) + (4-2\delta^2(1-a))z'^{-1} + \delta(1+\delta)(1-a)z'^{-2}}{(1-\delta) + 2\delta z'^{-1} - (1+\delta)z'^{-2}} \right] \Bigg|_{z'=e^{j\omega/r}} \quad (12)$$

The factor ' $r$ ' should be chosen for the minimum possible value of binary power to avoid clock synchronisation problem (Devate et al., 2015). Therefore, substitution of minimum possible integer  $r = 2$  and  $T = 1$  in Equations (11) and (12) yields the following  $F_1(z')$  and  $F_2(z')$ .

$$F_1(z') = \frac{(1+a)}{4} \left[ \frac{1 + \frac{1-a}{1+a}(1-\delta) + \frac{1-a}{1+a}\delta z'^{-1}}{1 - z'^{-1}} \right] \Bigg|_{z'=e^{j\omega/r}} \quad (13)$$

$$F_2(z') = \frac{1}{4} \left[ \frac{\delta(1-a)(\delta-1) + (4-2\delta^2(1-a))z'^{-1} + \delta(1+\delta)(1-a)z'^{-2}}{(1-\delta) + 2\delta z'^{-1} - (1+\delta)z'^{-2}} \right] \Bigg|_{z'=e^{j\omega/r}} \quad (14)$$

To get the first- and second-order transfer functions, the values of  $\delta$  and  $a$  in Equations (13) and (14) can be optimised.

Here,  $L_1$  based fitness function have been used instead of  $L_2$ -norm as it incorporates the drawbacks of obtaining high overshoots at discontinuous points and more ripples in the frequency response. Whereas  $L_1$  based fitness function provides a flatter filter response in both pass-band and stop-band (Aggarwal et al., 2017). Therefore, the error functions can be written as

$$E_1 = \sum |(|H_{int}(\omega)|) - |F_1(z')|_{z'=e^{j\omega/r}}| \quad (15)$$

$$E_2 = \sum |(|H_{int}(\omega)|) - |F_2(z')|_{z'=e^{j\omega/r}}| \quad (16)$$

Simulated annealing (SA) is a probabilistic technique which takes a population and applies a reducing random variation to each member of the population. It is a metaheuristic function to approximate global optimisation in a large search space for an optimisation problem, in which the rate and type of random variation are the part of the designing process (Bohachevsky et al., 1986). Therefore, application of the simulated

annealing (SA) optimisation algorithm (Bohachevsky et al., 1986) yields  $\delta = 0.62$ ,  $\alpha = 0.683$  for first-order and  $\delta = 0.9$ ,  $\alpha = 0.598$  for the second-order design. The first- and second-order transfer function of the proposed integrators are

$$F_1(z') = \left[ \frac{1.072z' + 0.1168}{2.377z' - 2.377} \right] \quad (17)$$

$$F_2(z') = \left[ \frac{0.03618z'^2 - 3.349z' - 0.6874}{-0.4z'^2 - 7.2z' + 7.6} \right] \quad (18)$$

#### 4. Simulation results

Figure 2 portrays the magnitude response of the proposed first- and second-order integrators along with the ideal. It is clearly seen from Figure 2, that both the designs show the correlated magnitude response with that of the ideal integrator. The magnitude response of the proposed-II design coincides with the ideal as compared to the proposed-I design in lower frequencies as can be seen in the zoomed region. Whereas in some part of high-frequency region the proposed-I design overlaps better than the proposed-II. The computed absolute magnitude error for the proposed designs over  $0.0314 \leq \omega \leq \pi$  are plotted in Figure 3. It depicts that, for the first-order integrator design, the absolute magnitude error remains less than  $0.38 \times 10^{-3}$  over  $0.13\pi \leq \omega \leq 0.76\pi$ . Whereas in

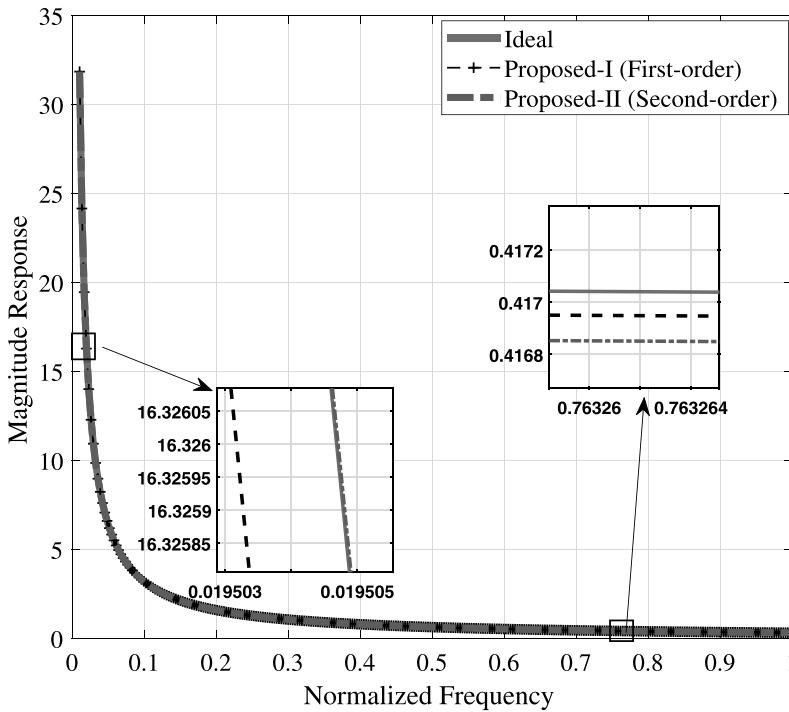
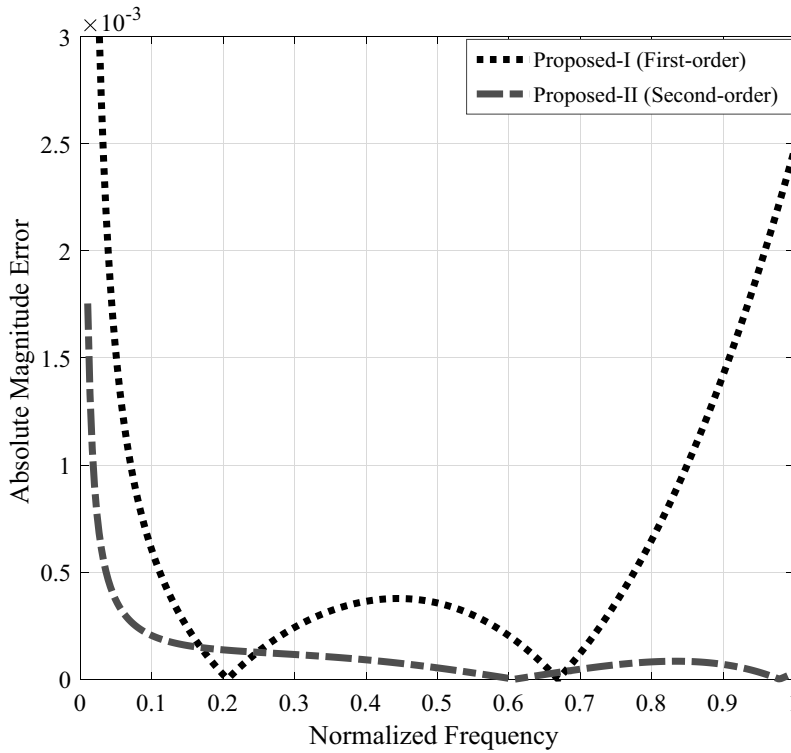


Figure 2. Magnitude response of proposed first-order and second-order digital integrators with ideal.



**Figure 3.** Absolute magnitude error of proposed first-order and second-order digital integrators.

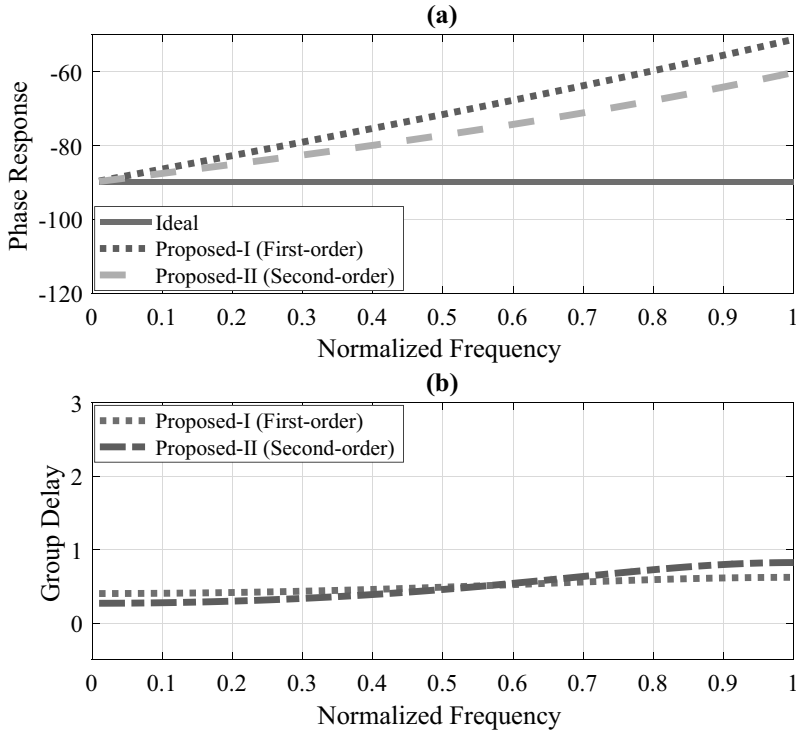
case of second-order design it remains less than  $0.25 \times 10^{-3}$  over  $0.1\pi \leq \omega \leq \pi$  and  $1.75 \times 10^{-3}$  over  $0.0314\pi \leq \omega \leq \pi$ .

Figure 4(a) shows the phase responses of the proposed designs along with the phase response of the ideal integrator. Both designs show a linear deviation with respect to the ideal. The first-order design shows the maximum deviation of 39.5 at  $\omega=\pi$ . Whereas in the case of second-order the maximum deviation is 29.5 at  $\omega=\pi$ . Figure 4(b) shows the group delay response of the proposed first- and second-order integrator design. Both designs show almost constant group delay with deviation between 0.2 and 0.8, which signifies the linearity of the phase.

## 5. Proposed design of the first- and second-order differentiators

The generalised transfer functions for the first- and second-order design of digital differentiator can be obtained by inverting the transfer function given in Equations (13) and (14) for the first-order and second-order respectively. Therefore, for  $r=2$  and  $T=1$ , the generalised equation for the first-order differentiator can be written as

$$F_{diff1}(z') = \frac{4}{(1+a)} \left[ \frac{1 - z'^{-1}}{1 + \frac{1-a}{1+a}(1-\delta) + \frac{1-a}{1+a}\delta z'^{-1}} \right] \bigg|_{z'=e^{j\omega/r}} \quad (19)$$



**Figure 4.** (a) Phase response of proposed first-order and second-order digital integrators with ideal (b) Group delay of proposed first-order and second-order digital integrators.

The generalised equation for the second-order integrator is obtained as

$$F_{diff2}(z') = 4 \left[ \frac{(1 - \delta) + 2\delta z'^{-1} - (1 + \delta)z'^{-2}}{\delta(1 - \alpha)(\delta - 1) + (4 - 2\delta^2(1 - \alpha))z'^{-1} + \delta(1 + \delta)(1 - \alpha)z'^{-2}} \right] \Bigg|_{z' = e^{j\omega/r}} \quad (20)$$

The optimisation is done to optimise the Equations (19) and (20) for the variables  $\delta$  and  $\alpha$ . The optimum values for  $\delta$  and  $\alpha$  are obtained as 0.29 and 0.294 respectively, with constant multiplier 0.997 for the first-order design and 0.898 and 0.593 respectively, with constant multiplier 1 for the second-order design. The first- and second-order transfer function of the proposed differentiators can be written as

$$F_3(z') = \left[ \frac{3.082z' - 3.082}{1.382z' + 0.1631} \right] \Bigg|_{z' = z^{1/2}} \quad (21)$$

$$F_4(z') = \left[ \frac{-0.408z'^2 - 7.184z' + 7.492}{0.03728z'^2 - 3.344z' - 0.6937} \right] \Bigg|_{z' = z^{1/2}} \quad (22)$$



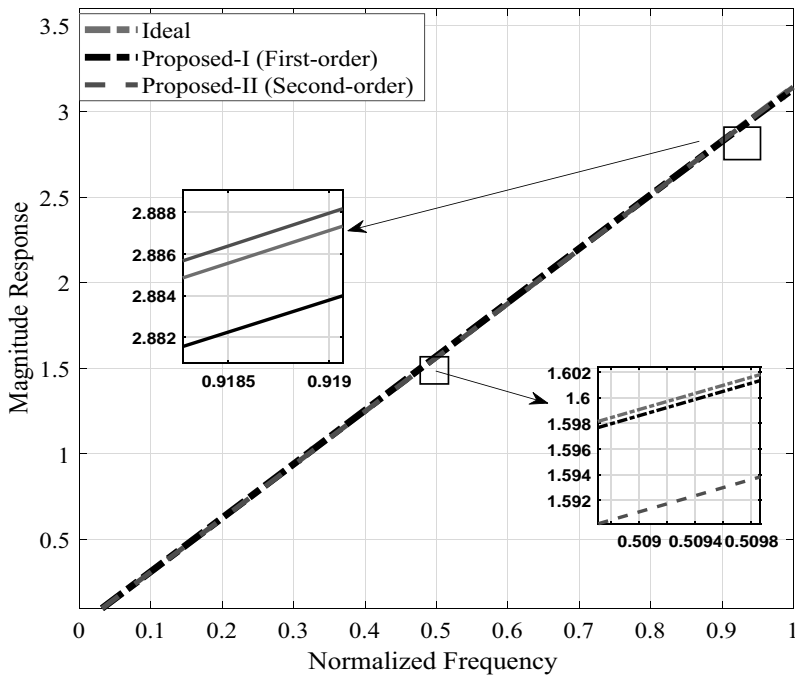


Figure 5. Magnitude response of proposed first-order and second-order digital differentiators with ideal.

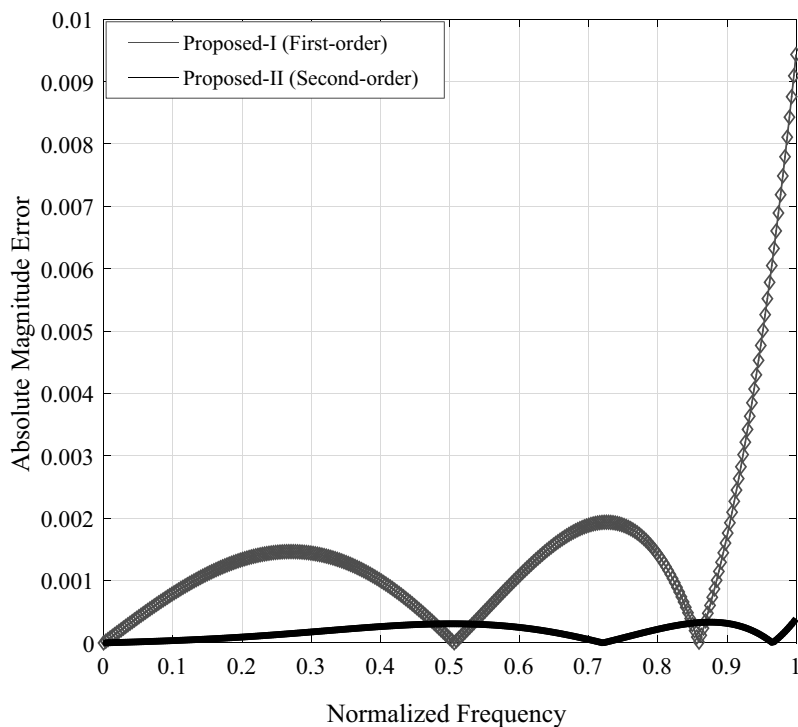
## 6. Simulation results

Figure 5 shows the magnitude response of the proposed first- and second-order differentiator. The absolute magnitude error of the proposed differentiators is shown in Figure 6. The magnitude response of the proposed designs overlaps with the magnitude response of the ideal differentiator. The zoomed frequency region shows that the first-order design provide less deviation than the second-order design in  $0.48\pi \leq \omega \leq 0.51\pi$  and  $0.84\pi \leq \omega \leq 0.86\pi$ . The absolute magnitude error remains less than 0.002 for  $0 \leq \omega \leq 0.87\pi$  and 0.01 for the entire Nyquist range. Whereas for the second-order design, the absolute magnitude error remains less than 0.00045 for  $0 \leq \omega \leq \pi$ .

Figure 7(a) presents the phase responses of the ideal and proposed designs of the digital differentiator. The first-order differentiator shows the linear phase with maximum deviation of  $39.5^\circ$  at  $\omega=\pi$ . Whereas the second-order differentiator design attains the linear phase with maximum deviation of  $29.85^\circ$  at  $\omega=\pi$ . Figure 7(b) shows the group delay response of the proposed first- and second-order differentiator design. Both designs show the group delay deviation between 0.25 and 0.78, which validates the linearity of the phase.

## 7. Comparison with the existing designs

In 2016, Devate et al. proposed the first-order differentiator and integrators derived from the natural logarithmic series. Further, their bandwidth was extended by using a simple multirate technique for different values of binary power  $r$  (Devate et al., 2015). A second-order integrator and differentiator was developed by Upadhyay by optimising the pole-



**Figure 6.** Absolute magnitude error of proposed first-order and second-order digital differentiators.

zero locations (Upadhyay, 2012). Another implementation of different order integrators and differentiators was suggested by Aggarwal et al. (Aggarwal et al., 2017). They optimised the  $L_1$ -error fitness function by employing the bat algorithm. The transfer functions of all these mentioned integrators and differentiators are enlisted in Table 1.

Figure 8 shows the comparison of the absolute magnitude error of the proposed digital integrators of first- and second-order, and the existing integrators, with the ideal for  $0.0314 \leq \omega \leq \pi$ . It is observed that the proposed-I integrator performs better than the designs proposed by Upadhyay, Aggarwal et al. and Devate et al. ( $r=8$ ) in a range of  $0.0314\pi \leq \omega \leq \pi$ . Though absolute magnitude error obtained by Devate et al. ( $r=16$ ) remains less than the proposed-I, yet it is for the higher value of  $r$ . Besides, the second-order proposed-II integrator outperforms all the mentioned designs for the entire Nyquist interval. The statistical results for integrators in Table 2 confirm the fact that the first-order proposed integrator shows the absolute relative magnitude error (ARME) (0.2100) and mean relative magnitude error (MRME) ( $-63.4393$  dB) than the others. A small difference is observed in ARME and MRME of the proposed-I integrator and Devate et al. ( $r=16$ ). However, proposed-II provides the least ARME (0.0359) and MRME ( $-78.771$  dB) as compared to all the integrators mentioned in Table 2.

Figure 9 presents the comparison of the absolute magnitude error of the proposed first- and second-order digital differentiators and the existing differentiators mentioned in Table 1. The proposed-I differentiator offers less magnitude error than designs proposed by the Upadhyay, Aggarwal et al. (second-order), Goswami et al. (second-order), Devate et al. ( $r=8$ ) and Devate et al. ( $r=16$ ) and shows the comparability with

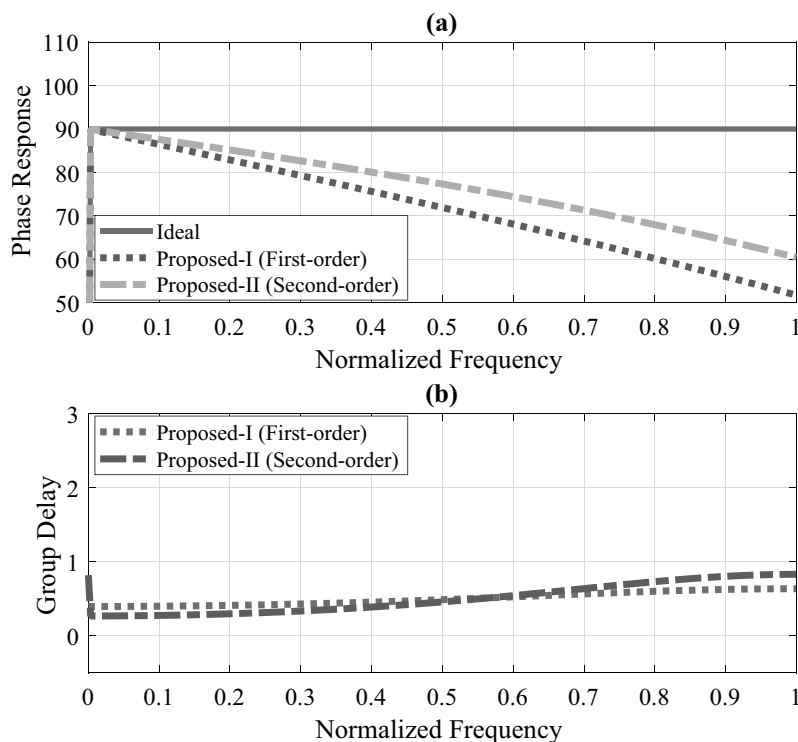


**Figure 7.** (a) Phase response of proposed first-order and second-order digital differentiators with ideal (b) Group delay of proposed first-order and second-order digital differentiators.

**Table 1.** Transfer functions of the existing integrators and differentiators using different technique.

| Technique     | Integrators   | Differentiators  |
|---------------|---|--|
| Multirate     | Devate et.al (first-order) ( $r = 8$ )<br>$\frac{T}{2r} \left( \frac{z+1}{z-1} \right) \Big _{z'=(z)^{1/r}}$  | Devate et.al (first-order) ( $r = 8$ )<br>$\frac{2r}{T} \left( \frac{z'-1}{z'+1} \right) \Big _{z'=(z)^{1/r}}$                     |
| Multirate     | Devate et.al (first-order) ( $r = 16$ )<br>$\frac{T}{2r} \left( \frac{z+1}{z-1} \right) \Big _{z'=(z)^{1/r}}$ | Devate et.al (first-order) ( $r = 16$ )<br>$\frac{2r}{T} \left( \frac{z'-1}{z'+1} \right) \Big _{z'=(z)^{1/r}}$                    |
| PZ            | Upadhyay (second-order)<br>$T \left( \frac{z^2+0.679z+0.0626}{1.1534z^2-0.5729z-0.58053} \right)$             | Upadhyay (second-order)<br>$\frac{1}{T} \left( \frac{1.1534z^2-0.5729z-0.58053}{z^2+0.679z+0.0626} \right)$                        |
| L1-BA         | Apoorva et al. (second-order)<br>$T \left( \frac{-0.5986z^2-0.4186z-0.0385}{0.694z^2-0.3275z-0.3569} \right)$ | Apoorva et al. (second-order)<br>$\frac{1}{T} \left( \frac{0.694z^2-0.3275z-0.3569}{-0.5986z^2-0.4186z-0.0385} \right)$            |
| L1-BA         |   | Apoorva et al. (third-order)<br>$\frac{1}{T} \left( \frac{0.2232z^3-0.2803z^2-0.4773}{0.4942z^3+0.6953z^2+0.2550z+0.0173} \right)$ |
| Interpolation |   | Goswami et al. (second-order)<br>$\frac{1}{T} \left( \frac{0.5048z^2+3.094z-3.599}{-3.106z^2-0.94899z+0.054276} \right)$           |

Aggarwal et al. (third-order), in the full Nyquist range. Whereas the proposed-II differentiator outperforms all the differentiators enlisted in Table 1. The statistical analysis of differentiators from Table 2 indicates the superiority of the proposed designs in terms of ARME and MRME. However, the calculated ARME and MRME for

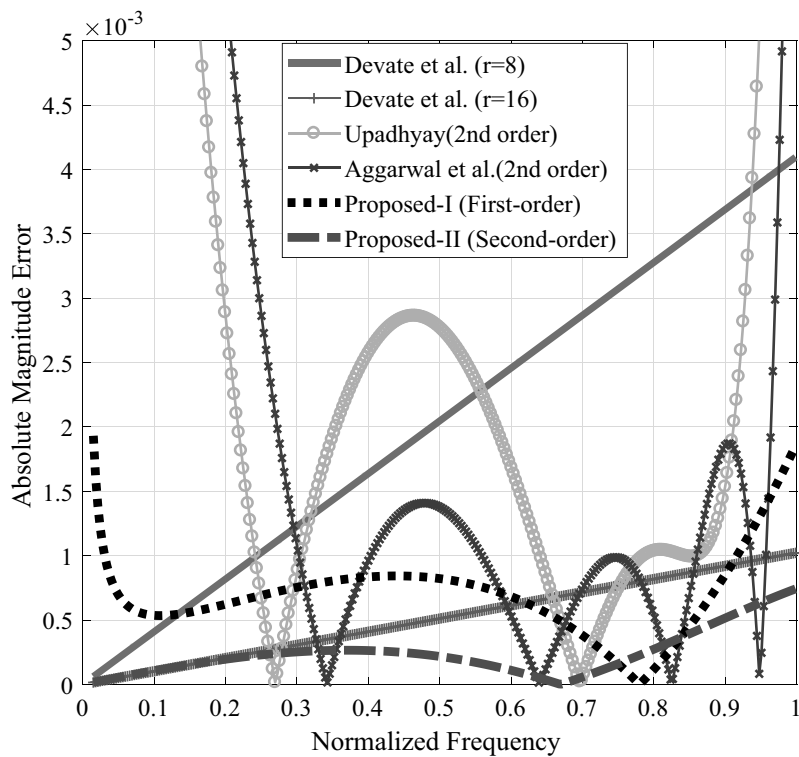


**Figure 8.** Magnitude response comparison of proposed digital integrators with existing designs.

**Table 2.** Statistical comparisons of proposed integrator and differentiator designs with their corresponding existing designs.

| Method                               | Integrators |           | Differentiators |           |
|--------------------------------------|-------------|-----------|-----------------|-----------|
|                                      | ARME        | MRME (dB) | ARME            | MRME (dB) |
| Devate et.al, (first-order) (r = 8)  | 0.6435      | −53.555   | 3.2178          | −39.827   |
| Devate et.al, (first-order) (r = 16) | 0.1607      | −65.7067  | 0.7982          | −52.041   |
| Upadhyay (second-order)              | 1.5985      | −45.679   | 2.9264          | −40.630   |
| Apoorva et al. (second-order)        | 1.5747      | −45.8485  | 1.6054          | −45.848   |
| Apoorva et al. (third-order)         | –           | –         | 0.3447          | −59.172   |
| Goswami et al. (second-order)        | –           | –         | 5.4927          | −35.04    |
| Proposed-I, (first-order) (r = 2)    | 0.2100      | −63.4393  | 0.4603          | −56.478   |
| Proposed-II, (second-order) (r = 2)  | 0.0359      | −78.771   | 0.0554          | −75.095   |

a proposed-I differentiator, are little more than the Aggarwal et al. (third-order) differentiator. Yet, the proposed-I (first-order) has a less order transfer function than of Aggarwal et al. (third-order). Furthermore, the second-order proposed-II differentiator shows the least ARME and MRME than the mentioned differentiators for the entire Nyquist range. Therefore, the proposed-I and Proposed-II may be regarded as a low order wideband digital differentiators.

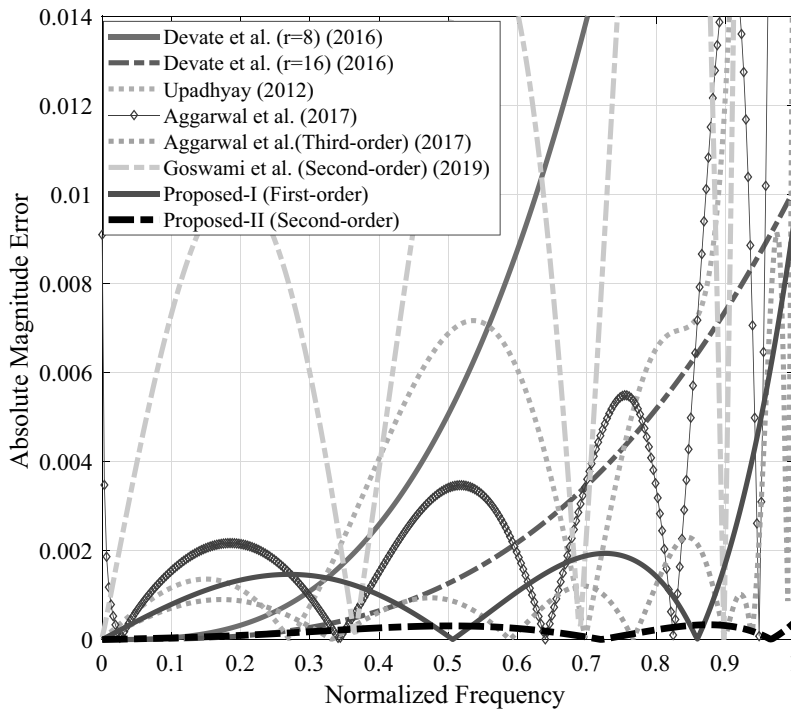


**Figure 9.** Magnitude response comparison of proposed digital differentiator with existing designs.

## 8. Conclusion

In this paper, the designs of the wideband digital integrators and differentiators have been proposed. The first- and second-order transfer functions of the digital integrator were obtained by applying the multirate technique to the fractional interpolation of the rectangular transform and bilinear transform. Thereafter, it is followed by the optimisation of two variables, namely, fractional delay variable  $\delta$  and weighting variable  $\alpha$ . By inverting their generalised transfer function followed by the optimisations, the designs of digital differentiators were obtained. The proposed designs are compared with the existing designs to demonstrate their supremacy. Therefore, these low order wideband proposed digital integrators and digital differentiators may be used as an alternative to the existing ones and preferred for the real-time applications.

## Disclosure statement

No potential conflict of interest was reported by the authors.

## References

- Aggarwal, A., Rawat, T. K., & Upadhyay, D. K. (2017). Optimal design of  $L_1$ -norm based IIR digital differentiators and integrators using the bat algorithm. *IET Signal Processing*, 11(1), 26–35.9. <https://doi.org/10.1049/iet-spr.2016.0010>

- Al-Alaoui, M. A. (1992). Novel approach to designing digital differentiators. *Electronics Letters*, 28(15), 1376–1378. <https://doi.org/10.1049/el:19920875>
- Al-Alaoui, M. A. (1993). Novel digital integrator and differentiator. *Electronics Letters*, 29(4), 376–378. <https://doi.org/10.1049/el:19930253>
- Al-Alaoui, M. A. (1994). Novel IIR differentiator from the Simpson integration rule. *IEEE Transactions on Circuits and Systems I: Fundamental Theory and Applications*, 41(2), 186–187. <https://doi.org/10.1109/81.269060>
- Al-Alaoui, M. A. (2011). Class of digital integrators and differentiators. *IET Signal Processing*, 5(2), 251–260. <https://doi.org/10.1049/iet-spr.2010.0107>
- Al-Alaoui, M. A., & Baydoun, M. (2013). Novel wide band digital differentiators and integrators using different optimization techniques. *International Symposium on Signals, Circuits and Systems (ISSCS2013)* (pp. 1–4).
- Bohachevsky, I. O., Johnson, M. E., & Stein, M. L. (1986). Generalized simulated annealing for function optimization. *Technometrics*, 28(3), 209–217. <https://doi.org/10.1080/00401706.1986.10488128>
- Devate, J., Kulkarni, S. Y., & Pai, K. R. (2014). Wideband IIR digital integrator and differentiator. *Proceedings of International Conference on Circuits, Communication, Control and Computing* (pp. 81–84).
- Devate, J., Kulkarni, S. Y., & Pai, K. R. (2015). Wideband differentiator and integrator with ideal phase response. *Canadian Journal of Electrical and Computer Engineering*, 38(4), 294–299. <https://doi.org/10.1109/CJECE.2015.2444443>
- Dyer, S. A., & Dyer, J. S. (2000). The bilinear transformation. *IEEE Instrumentation & Measurement Magazine*, 3(1), 30–34. <https://doi.org/10.1109/5289.823821>
- Goswami, O. P., Rawat, T. K., & Upadhyay, D. K. (2019). Fractional bilinear transform based design of wideband digital differentiator using multirate technique. *5th International Conference on Signal Processing, Computing and Control (ISPCC)* (pp. 372–375). India.
- Goswami, O. P., Rawat, T. K., & Upadhyay, D. K. (2020). A novel approach for the design of optimum IIR differentiators using fractional interpolation. *Circuits Systems and Signal Processing*, 39(3), 1688–1698. <https://doi.org/10.1007/s00034-019-01211-0>
- Gupta, M., Jain, M., & Kumar, B. (2010a). Novel class of stable wideband recursive digital integrators and differentiators. *IET Signal Processing*, 4(5), 560–566. <https://doi.org/10.1049/iet-spr.2009.0030>
- Gupta, M., Jain, M., & Kumar, B. (2010b). Recursive wideband digital integrator and differentiator. *International Journal of Circuit Theory and Applications*, 39(7), 775–782. <https://doi.org/10.1002/cta.658>
- Jang, Y. K., & Chicharo, J. F. (1993). Adaptive IIR comb filter for harmonic signal cancellation. *International Journal of Electronics*, 75(2), 241–250. <https://doi.org/10.1080/00207219308907103>
- Laakso, T. I., Valimäki, V., Karjalainen, M., & Laine, U. K. (1996). Splitting the unit delay: Tools for fractional delay filter design. *IEEE Signal Processing Magazine*, 13(1), 30–60. <https://doi.org/10.1109/79.482137>
- Liu, S. I., Chen, C. H., Tsao, H. W., & Wu, J. (1991). Switched-current differentiator-based IIR and FIR filters. *International Journal of Electronics*, 71(1), 81–91. <https://doi.org/10.1080/00207219108925460>
- Mishra, S. K., Upadhyay, D. K., & Gupta, M. (2019). Search of optimal s-to-z mapping function for IIR filter designing without frequency pre-warping. *IETE Journal of Research*, 1–9. <https://doi.org/10.1080/03772063.2019.1569484>
- Ngo, N. Q. (2006). A new approach for the design of wideband digital integrator and differentiator. *IEEE Transaction on Circuits and Systems II: Express Briefs*, 53(9), 936–940. <https://doi.org/10.1109/TCSII.2006.881806>
- Oppenheim, A. V., Schaffer, R. W., & Buck, J. R. (1999). *Discrete-time signal processing*. Prentice Hall.
- Pei, S. C., & Hsu, H. J. (2008). Fractional bilinear transform for analog-to-digital conversion. *IEEE Transaction on Signal Processing*, 56(5), 2122–2127. <https://doi.org/10.1109/TSP.2007.912250>
- Stani, G., Krsti, I., & Cvetkovi, S. (2020). All-pass-based design of nearly-linear phase IIR low-pass differentiators. *International Journal of Electronics*. <https://doi.org/10.1080/00207217.2020.1726498>
- Tsai, J. T., Chou, J. H., & Liu, T. K. (2006). Optimal design of digital IIR filters by using hybrid taguchi genetic algorithm. *IEEE Transaction on Industrial Electronics*, 53(3), 867–879. <https://doi.org/10.1109/TIE.2006.874280>
- Upadhyay, D. K. (2010). Recursive wideband digital differentiator. *Electronics Letters*, 46(25), 1661–1662. <https://doi.org/10.1049/el.2010.2113>

- Upadhyay, D. K. (2012). Class of recursive wideband digital differentiators and integrators. *Radioengineering*, 21(3), 904–910.
- Upadhyay, D. K., & Singh, R. K. (2011). Recursive wideband digital differentiator and integrator. *Electronics Letters*, 47(11), 647–648. <https://doi.org/10.1049/el.2011.0420>
- Xu, Y., Dai, T., Sycara, K. P., & Lewis, M. (2010). Service level differentiation in multi-robots control. *IEEE/RSJ International Conference on Intelligent Robots and Systems* (pp. 2224–2230).